



14 **Abstract**

15 Conventionally, subsurface fluid flow modelling studies have concentrated on the  
16 characterization of fracture networks and their capacity to facilitate vertical and lateral fluid  
17 movements. This study utilizes unique field observations of oxidation halos in a well-bedded  
18 carbonate sequence in the Paris Basin, France, offering new perspectives on fluid flow  
19 pathways. It demonstrates that, in addition to fractures, bedding planes also serve as critical  
20 conduits for horizontal fluid flow. This research highlights the importance of integrating both  
21 fractures and bedding planes to assess connectivity and therefore improve fluid flow models,  
22 especially in sedimentary basins. This approach is vital for geoscience and engineering  
23 applications, including reservoir management and waste disposal strategies.

24

25 **1 Introduction**

26 In tightly cemented sedimentary rocks, fractures are widely recognized as the primary  
27 conduits for fluid flow, especially in environments where matrix permeability is low (Nelson,  
28 1985). Consequently, common approaches to predicting subsurface fluid migration have  
29 predominantly focused on characterizing fracture networks (Bourbiaux, 2010; De Dreuzy et al.,  
30 2012; Lei et al., 2017). Conventionally, outcrop-scale data is utilized to inform larger-scale  
31 subsurface flow models by assessing the geometric and topological properties of these fracture  
32 networks (Odling et al., 1999; Agosta et al., 2010; Sanderson and Nixon, 2015; Wennberg et al.,  
33 2016; Lei et al., 2017). These properties, typically measured directly at the outcrop scale, help  
34 estimate the extent and scaling of these networks in the subsurface, thereby constraining flow  
35 properties (Wilson et al., 2011; Zhu et al., 2021).

36 However, this well-established approach assumes that subsurface fluid flow is primarily  
37 accommodated by fracture networks, which predominantly facilitate vertical and lateral fluid  
38 movements. Consequently, it often neglects the potential for horizontal fluid movements that  
39 could be facilitated, for example, by bedding planes—stratigraphic layers and/or interfaces  
40 between layers. This neglect is largely due to the challenges associated with identifying these

41 horizontal fluid flow pathways, leading to an exclusive focus on fractures as the main conduits  
42 for fluid flow.

43 The primary goal of this study is to highlight the often-overlooked importance of  
44 bedding planes in fluid flow. Field observations from an exceptional exposure of oxidation halos  
45 within a well-bedded carbonate sequence in the Paris Basin, France, provide critical insights  
46 into past fluid flow pathways. Results suggest that bedding planes also play a crucial role as  
47 pathways, and their interaction with sub-vertical fractures enhance the overall connectivity of  
48 fluid systems. This finding highlights the necessity of integrating both fractures and bedding  
49 planes into subsurface fluid flow models, especially in well-bedded sedimentary sequences.  
50 Incorporation of bedding planes into flow models can therefore improve our understanding of  
51 subsurface fluid dynamics, which is essential for various geoscientific and engineering  
52 applications, including efficient reservoir management and waste disposal strategies (e.g., Bear  
53 et al., 2012).

## 54 **2 Data and Methodology**

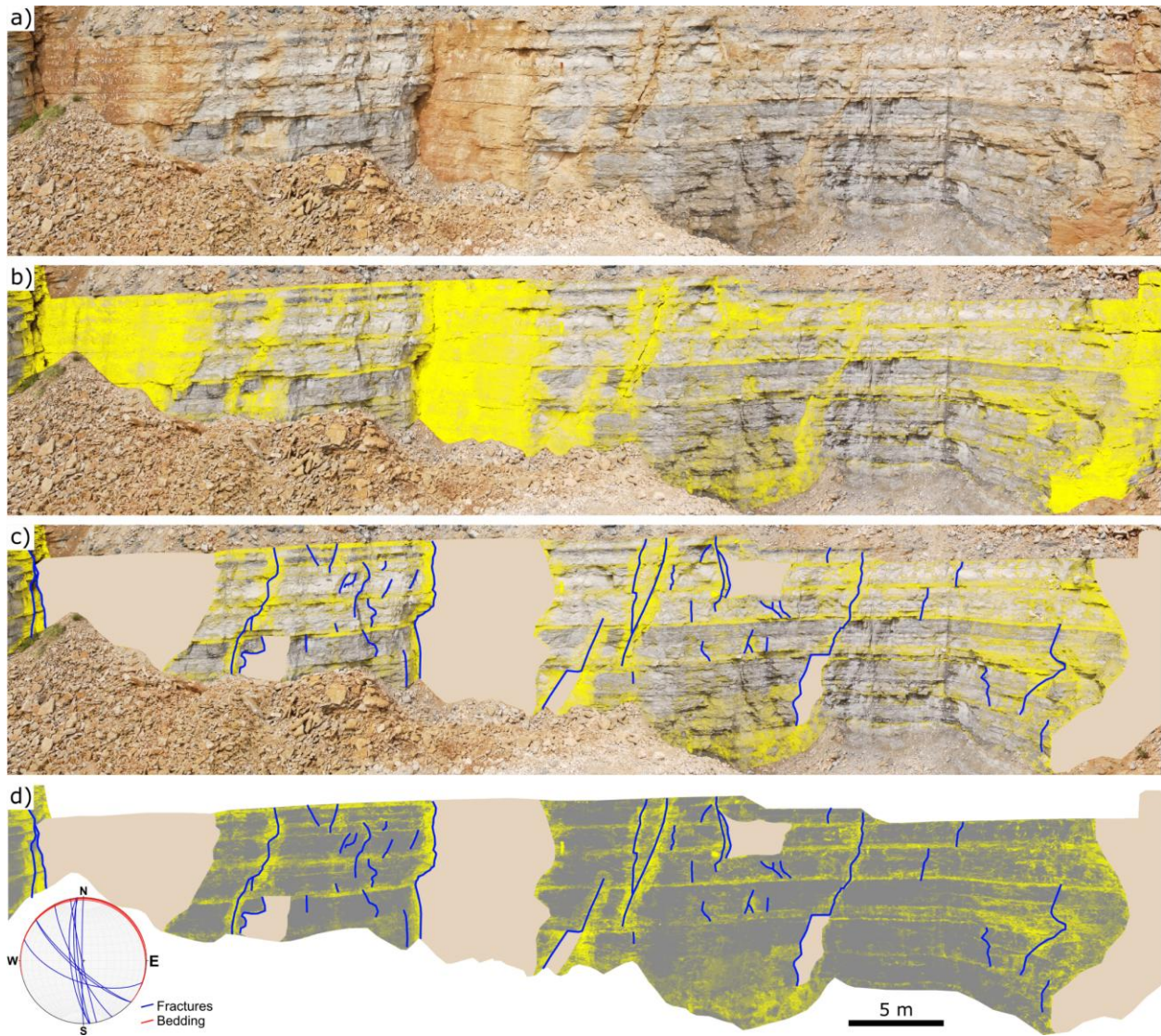
55 The study is based on an outcrop exposure within the Sommerécourt quarry at the  
56 eastern Paris Basin, France. The Paris Basin is an intracratonic basin that experienced multiple  
57 episodes of subsidence and sedimentation during the Mesozoic (Pomerol, 1978; Mégnien,  
58 1980). This study focuses on the Dogger Formation, primarily composed of limestone and marl,  
59 deposited during the Middle Jurassic and marking a transition from marine transgression to  
60 more restricted lagoonal conditions (e.g., Brigaud et al., 2009). The formation is extensively  
61 studied for its petroleum potential and geothermal resources in the Paris Basin (e.g., Lopez et  
62 al., 2010) and its western continuation in the Upper Rhine Graben (e.g., Böcker et al., 2017).

63 On a more regional scale, the outcrop is located approximately 200 meters north of the  
64 E-W striking Vittel fault, which forms part of the extensive Variscan Wight-Bray-Vittel  
65 megastructure, extending over 700 km from the Bristol Channel to eastern France. This major  
66 tectonic structure was reactivated during the Meso-Cenozoic period (Bergerat et al., 2007) and  
67 has been reported as a major corridor for paleo-circulation of geothermal fluids within the Paris  
68 Basin, facilitating connections between the Dogger and Triassic reservoirs (Bril et al., 1994).

69 In the studied outcrop, fractures exhibit approximately NW-SE strikes, with an average  
70 dip of 80°, while the bedding planes are nearly horizontal, dipping on average 3° towards the  
71 NNE (as shown in the inset in Figure 1). Oxidation halos, which serve as key indicators of past  
72 fluid flow, are observed surrounding both fractures and bedding planes (Figure 1). A cut surface  
73 of a rock sample and a thin section illustrating the oxidation halo in contrast to the non-  
74 oxidized host rock are presented in Figure 2. This figure clearly shows the sharp transition from  
75 the orange to reddish-brown hues of the oxidized zone to the greyish-blue and beige tones of  
76 the non-oxidized host rock, further confirming the presence and intensity of oxidation halos at  
77 a finer scale.

78 To enhance the examination of these halos, field observations were supplemented with  
79 image processing techniques to improve their visibility. A virtual outcrop model (VOM) and a 2D  
80 orthorectified image of the quarry working face were created from digital images collected by  
81 an unmanned aerial vehicle (UAV). Subsequently, Inkscape software was used to apply a  
82 fluorescence filter to increase the contrast between the halos and the surrounding rock matrix,  
83 allowing for the detection of subtle oxidation variations that might otherwise go unnoticed.  
84 Additionally, a saturation map filter was used to adjust colour intensities, further enhancing the  
85 clarity of the halos. These image manipulations, combined with adjustments to contrast and  
86 brightness, enabled more precise identification of the halos and allowed for detailed mapping  
87 of both fractures and bedding planes that facilitated past fluid flow (Figures 1 and 3).

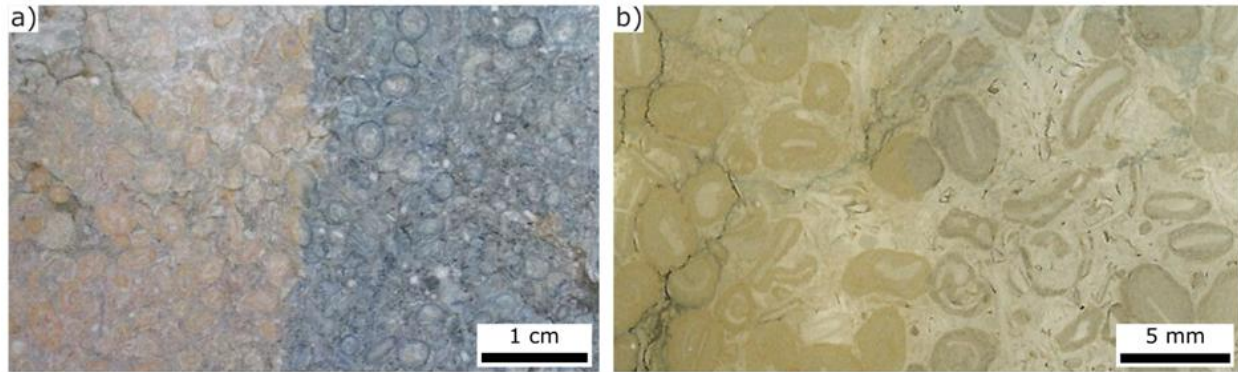
88 The resulting maps were used to analyse the connectivity and estimate the intensity and  
89 density of fractures and bedding planes. Connectivity analysis involved mapping the spatial  
90 distribution of three node types, as defined by Manzocchi (2002): isolated tips (I-nodes),  
91 crossing fractures/bedding planes (X-nodes), and abutments or splays (Y-nodes). The  
92 terminology by Dershowitz and Herda (1992) is followed for the intensity of fractures and/or  
93 bedding planes (P21), which is defined as the length per unit area, and their density (P20),  
94 which is defined as the number of features per unit area. These metrics were calculated using  
95 the method of Mauldon et al. (2001) and implemented with FracPac v. 2.8 (Healy et al., 2017).



96

97 **Figure 1.** (a) Panoramic view of the studied outcrop. (b) Image processing enhances the visibility  
98 of oxidation halos, highlighted in yellow. (c) Fracture traces are shown in blue, while fracture  
99 surfaces are marked in brown. (d) Same as (c), but without the original image background. The  
100 inset shows the orientation of fractures and bedding planes as great circles on a lower  
101 hemisphere, equal-area projection.





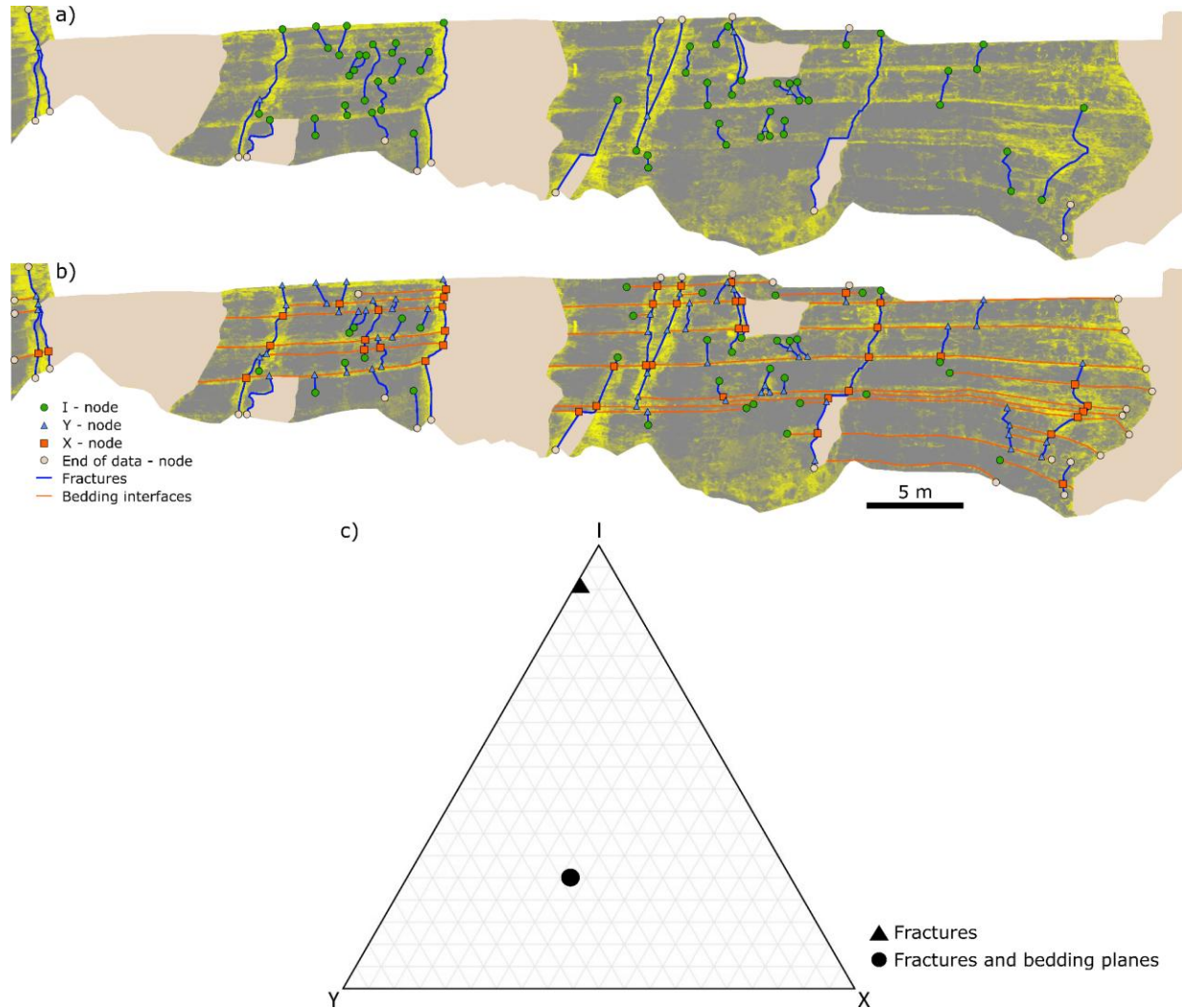
102

103 **Figure 2.** (a) Cut surface of the rock sample and (b) thin section showing both the oxidation halo  
104 (left side) and the non-oxidized host rock (right side). A sharp transition from the orange to  
105 reddish-brown hues of the oxidized zone to the grayish-blue and beige tones of the non-  
106 oxidized host rock is observed.

### 107 **3 Results**

108 This section highlights the critical importance of integrating both fractures and bedding  
109 planes when analyzing fluid flow in sedimentary formations. Figure 3 (a and b) presents  
110 connectivity maps comparing two different scenarios: (a) fractures only, and (b) both fractures  
111 and bedding planes. These maps clearly demonstrate a marked increase in connectivity when  
112 bedding planes are considered alongside fractures. Furthermore, Figure 3c shows a ternary plot  
113 based on I-Y-X connectivity analysis (Manzocchi, 2002), comparing the fracture network alone  
114 (from Figure 3a) with the combined network of fractures and bedding planes (from Figure 3b).  
115 Networks showing improved connectivity are positioned towards the base of the triangle,  
116 indicating a higher proportion of X and Y nodes. This shift towards the base in the combined  
117 network plot highlights the enhanced connectivity provided by bedding planes, demonstrating  
118 quantitatively how their inclusion can lead to more efficient fluid flow within the well-bedded  
119 sedimentary sequence. This enhanced connectivity not only supplements the vertical pathways  
120 provided by fractures but also introduces vital horizontal routes that could facilitate broader  
121 fluid distribution across the formation. This effectively links isolated fractures, turning bedding  
122 planes into critical conduits that increase overall system connectivity. It is worth noting,  
123 however, that the aforementioned connectivity properties of the fracture network primarily  
124 reflect only the vertical direction, influenced by the nature of the available data (e.g., cross-

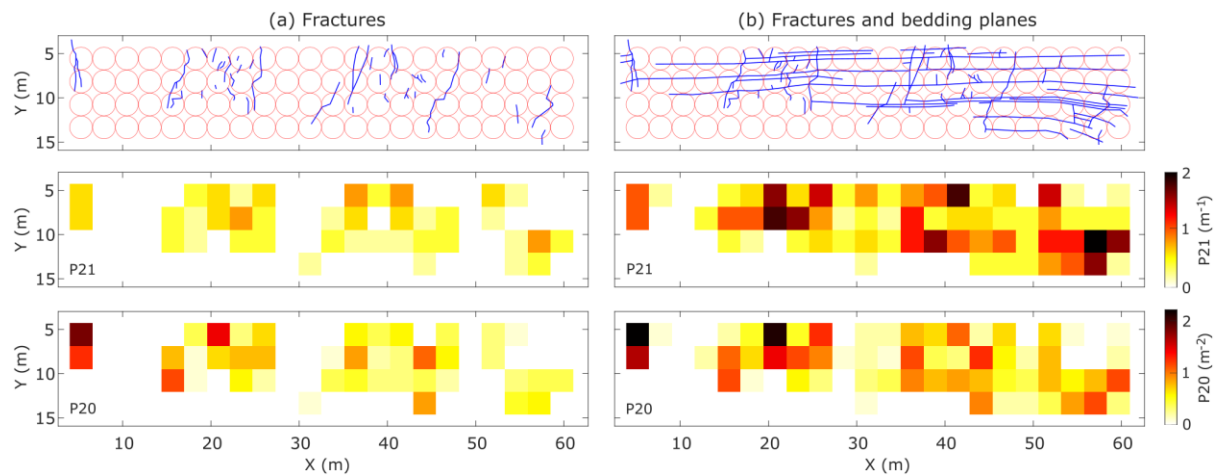
125 sectional view of the quarry face). However, given the measured orientations of fractures (as  
126 shown in the inset of Figure 1), the fracture network is expected to exhibit lateral connectivity,  
127 which would further facilitate lateral fluid movements.



128

129 **Figure 3.** Connectivity maps showing the spatial distribution of different node types (I, Y and X)  
130 for (a) fractures only, and (b) both fractures and bedding planes at the studied outcrop. (c)  
131 Ternary plot of I-Y-X connectivity analysis (Manzocchi, 2002) comparing the fracture network  
132 alone (as in a) with the combined fracture and bedding plane network (as in b) at the studied  
133 outcrop. Better-connected networks are plotted toward the base of the triangle indicating a  
134 higher proportion of X and Y nodes.

135 Maps of the estimated intensity and density of (a) fractures only and (b) both fractures  
 136 and bedding planes are presented in Figure 4. These maps indicate that areas with combined  
 137 fracture and bedding plane networks have higher P21 and P20 values, suggesting a denser and  
 138 potentially more permeable structure conducive to fluid migration. These parameters are  
 139 crucial as they directly influence the fluid flow properties of the formation, with higher values  
 140 generally indicative of increased potential for fluid storage and transport. Complementing the  
 141 connectivity maps shown in Figure 3, these P21 and P20 maps further demonstrate how  
 142 apparently isolated fracture corridors become interconnected through fluid flow along the  
 143 bedding planes.

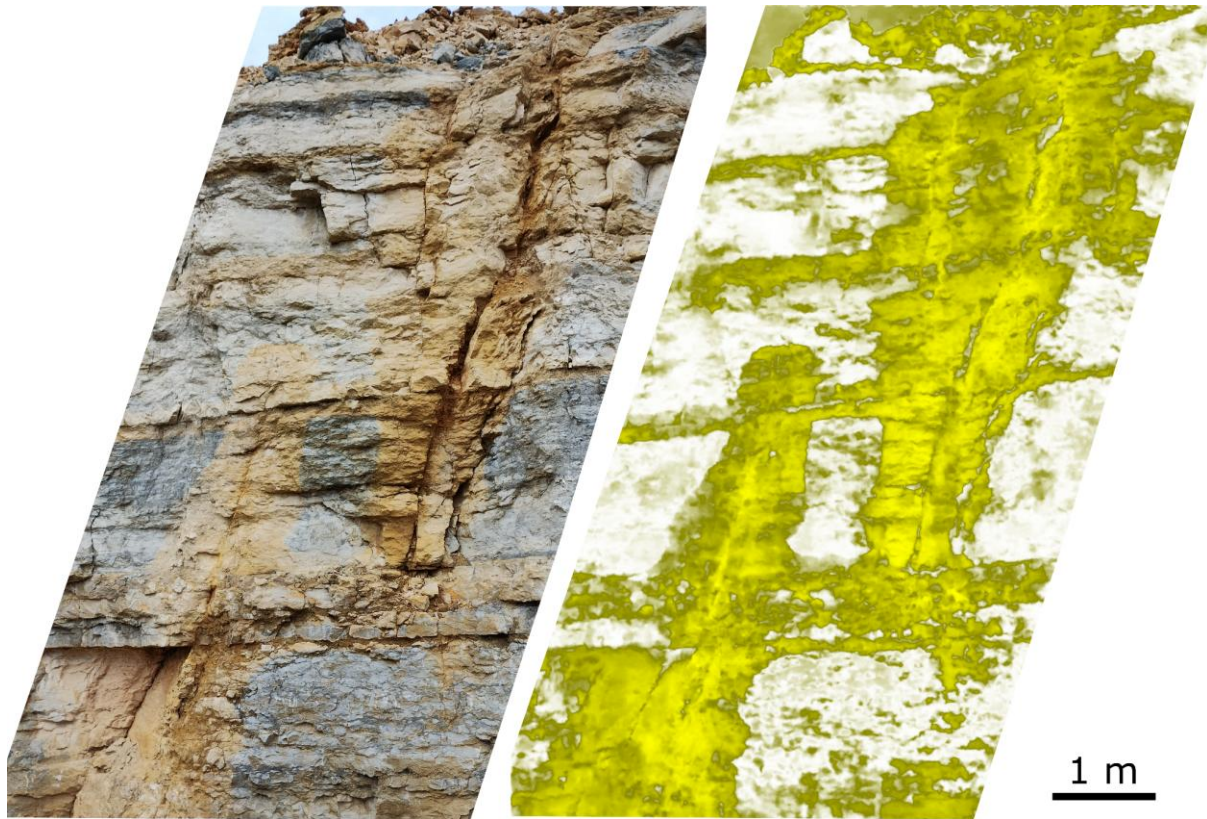


144  
 145 **Figure 4.** Estimated fracture intensity (P21) and fracture density (P20) maps for (a) fractures  
 146 only, and (b) both fractures and bedding planes at the studied outcrop. Fracture traces and  
 147 fracture plus bedding plane traces (depicted in blue) are shown at the top, indicating the  
 148 locations of the scan circles used to estimate intensity ( $\text{m}^{-1}$ ) and density ( $\text{m}^{-2}$ ).

149 While this study demonstrates that bedding planes can serve as horizontal pathways for  
 150 fluid flow, they also have the capacity to restrict both fracture propagation and associated  
 151 vertical fluid movements. In Figure 5, the fracture on the right and its associated oxidation halo  
 152 terminate abruptly at a bedding plane, acting as a barrier to fluid migration below this plane  
 153 and to downward fracture propagation. Despite this abrupt termination, the presence of the  
 154 halo along the corresponding bedding plane indicates fluid flow along it, resulting in a Y-node  
 155 connection as shown in Figure 3. Conversely, the fracture on the left is not restricted by any



156 bedding plane, and its associated halo gradually terminates upwards, becoming well-rounded  
157 at the fracture tip. These observations, further highlight the well-documented influence of  
158 mechanical stratigraphy on fracture propagation across different bedding planes (e.g., Renshaw  
159 and Pollard, 1995; McGinnis et al., 2017), illustrating the complex interplay between bedding  
160 planes, fracture growth, and fluid dynamics.



161  
162 **Figure 5.** Close-up photograph of the outcrop on the left, and the same image after processing  
163 to enhance the visibility of oxidation halos, which are highlighted in yellow on the right.

#### 164 **4 Discussion**

##### 165 4.1 Factors controlling fluid flow along bedding planes

166 Through semi-quantitative analysis involving geometrical and topological assessments,  
167 this study demonstrates that bedding planes not only complement the vertical and lateral fluid  
168 pathways provided by fractures but also significantly enhance system connectivity through  
169 horizontal routes.

170           The factors controlling fluid flow along bedding planes in the studied area have not yet  
171 been fully identified. However, preliminary observations suggest that dissolution processes,  
172 particularly pressure-solution of the cement between detrital and precipitated grains, are likely  
173 responsible for the development of porosity and permeability within the marly limestone  
174 layers.

175           Previous research on fluid flow along bedding planes, although less common than  
176 studies on fractures, primarily focuses on phenomena such as karstification and cave genesis  
177 (Cooke et al., 2006; Filipponi et al., 2010; Sauro et al., 2013; Frumkin et al., 2017; Roded et al.,  
178 2024). For example, Filipponi et al. (2010) identified three distinct types of inception horizons  
179 that promote cave development and, consequently, concentrate fluid flow. These types are  
180 differentiated by differences in permeability and the presence of fractures along bedding  
181 interfaces. Additionally, Sauro et al. (2013) reported that flexural slip surfaces between beds  
182 are particularly conducive to the development of conduits and deep karst systems. In another  
183 study focusing on hydrocarbon migration, Noufal and Obaid (2017) noted that sheared bedding  
184 planes acted as primary corridors in the migration of hydrocarbons within Abu Dhabi's  
185 sedimentary basins. Furthermore, Skurtveit et al. (2021) found that the fractures along bedding  
186 interfaces and the petrophysical properties of the rock sequence-controlled layer-parallel CO<sub>2</sub>  
187 migration away from fault zones, which serve as the main pathways for CO<sub>2</sub> migration in  
188 Humbug Flats, Utah, USA. A recurrent theme in all these studies is the role of shearing and  
189 fracturing along bedding interfaces in promoting bed-parallel fluid flow. Given that bed-parallel  
190 shearing is quite commonly observed in both compressional (e.g., Sanderson, 1982; Tanner,  
191 1989) and extensional (e.g., Delogkos et al., 2022) tectonic settings, it is plausible that such  
192 shearing can also enhance fluid flow along these bedding planes.

193           Other factors reported to promote fluid flow along bedding planes include differences in  
194 the petrophysical properties between different layers such as permeability (e.g., Filipponi et al.,  
195 2010) and sedimentological processes. For example, Cooke et al. (2006) concluded that  
196 continuous flow along bedding planes may promote dissolution, which over time could lead to  
197 development of regionally extensive, bed-parallel, high-permeability features. Frumkin et al.  
198 (2017) also observed that bedding planes can initially have sub-millimetre to sub-centimetre

199 width, which subsequently increases due to dissolution enlargement. Furthermore, Golab et al.  
200 (2017) reported that bioturbation-influenced porosity enhances horizontal fluid flow within a  
201 carbonate platform system in otherwise low porosity and permeability sediments. Finally, it is  
202 worth mentioning that horizontal fluid flow pathways can be highly variable in three  
203 dimensions due to the inherent variability of petrophysical and sedimentological properties.  
204 Thomas et al. (2021) demonstrated the presence of such three-dimensional heterogeneities of  
205 facies, porosity, and permeability within the Middle Jurassic carbonate reservoirs in Paris Basin.

206 Additionally, the presence of karstification features in the examined area is noteworthy,  
207 as it can significantly influence subsurface fluid flow by potentially complicating pre-existing  
208 pathways and enhancing permeability and connectivity (e.g., Moore and Walsh, 2021). This  
209 highlights the complex, multifaceted nature of fluid flow in the subsurface and emphasizes the  
210 necessity of integrating various geological features and processes in subsurface flow modelling -  
211 an aspect often underestimated in prior studies.

#### 212 4.2 Conditions of formation of oxidation halos

213 Oxidation halos are typically associated with shallow subsurface conditions, where  
214 oxidizing fluids circulate, but their depth range can vary depending on the fluid source and  
215 redox conditions. In most cases, oxidation halos form due to meteoric groundwater infiltration,  
216 generally within the upper few hundred meters of the subsurface (0–500 m). However,  
217 oxidation at greater depths can also occur when oxidized fluids originate from deep-seated  
218 reservoirs, such as hydrothermal systems or basinal brines (e.g., Grare et al., 2018).

219 In the studied area, XRF measurements of rock samples indicate that iron content  
220 remains similar in both the oxidized zone and the host rock, with values ranging between 7000  
221 and 8000 ppm. This suggests that iron was not significantly leached or transported, but rather  
222 that oxygen introduced through meteoric groundwater infiltration converted  $\text{Fe}^{2+}$  to  $\text{Fe}^{3+}$  in situ  
223 at relatively shallow depths.

224 Although oxidation halos can, in certain settings, form under stagnant water conditions  
225 (Balsamo et al., 2013), observations in the studied area suggest a different scenario. The  
226 oxidation halos exhibit elongated and interconnected patterns that align with structural

227 discontinuities, such as bedding planes and fractures. This geometry, which reflects structural  
228 anisotropy, is more characteristic of advective flow pathways, where fluids migrate through  
229 preferential conduits rather than diffusing isotropically in stagnant conditions.

230 Furthermore, if oxidation had occurred under fully stagnant conditions, Fe oxidation  
231 would be expected to be uniform throughout the rock mass. However, XRF measurements  
232 indicate that iron content remains similar across the entire rock mass, confirming that iron was  
233 not leached or transported in significant amounts. The fact that oxidation is localized along  
234 fractures and bedding planes suggests that an oxidizing (O-rich) fluid must have circulated  
235 advectively, even if the surrounding rock was immersed in a stagnant, reduced water  
236 environment.

237 Future geochemical and isotopic analyses could further refine this interpretation and  
238 provide a more detailed understanding of the fluid origins and migration history.

#### 239 4.3 Implications

240 Although, the examined oxidation halos are potentially associated with near-surface  
241 conditions, the fundamental processes governing fluid flow, connectivity, and permeability are  
242 not necessarily depth-dependent. The oxidation halos in our study serve as natural tracers of  
243 paleo-fluid pathways, providing direct evidence of preferential flow along bedding planes. This  
244 has implications for deeper subsurface reservoirs, where similar structural and stratigraphic  
245 controls on fluid migration can be expected. Therefore, despite the shallow setting of our  
246 dataset, the observed fluid flow patterns provide insights into permeability anisotropy, which  
247 can be extrapolated to deeper subsurface environments, where direct observations are  
248 inherently limited.

249 The findings of this study, therefore, can have significant implications for various  
250 subsurface activities. Reservoir models that focus exclusively on fractures may underestimate  
251 fluid storage and transport potential, potentially leading to suboptimal decisions in reservoir  
252 management or waste disposal. By incorporating bedding planes into fluid flow models,  
253 predictions of fluid movement in reservoirs and aquifers can become more accurate, which is  
254 crucial for effective (a) resource extraction, including groundwater, geothermal energy, and

255 hydrocarbons, and (b) environmental management, such as carbon capture and storage (CCS)  
256 and contamination control. For example, in geothermal energy production, understanding the  
257 dual role of fractures and bedding planes can refine recovery strategies by optimizing well  
258 placements and enhancing recovery methods. This is particularly valuable for the Paris Basin,  
259 known for its geothermal energy resources, as well as for other basins where the Dogger  
260 Formation is present and exhibits high geoenergy potential, such as the Upper Rhine Graben.  
261 Furthermore, the findings of this study can contribute to a deeper understanding of  
262 fundamental geological processes such as karstification, speleogenesis, and diagenesis,  
263 advancing our knowledge of their development and distribution.

## 264 **5 Conclusions**

265         The examination of the exceptionally well exposed oxidation halos within the well-  
266 bedded carbonate sequence in the Paris Basin, France, reveals that subsurface fluid flow is  
267 more complex than previously understood. This study demonstrates that fluids can  
268 preferentially flow horizontally along bedding planes, complementing vertical and lateral flows  
269 along fracture networks. Bedding planes thus can act as critical conduits for fluid migration,  
270 especially in regions with low fracture density or poorly connected fractures. This challenges  
271 the conventional focus solely on fractures and highlights the need for bedding planes to be  
272 more thoroughly considered in fluid flow models.

273

## 274 **Acknowledgments**

275 This work was supported by a French government grant managed by the Agence Nationale de  
276 la Recherche under the France 2030 initiative, reference ANR-22-EXSS-0010. The authors would  
277 like to extend their gratitude to Guy Calin for granting permission to conduct research in the  
278 quarry, and to the quarry employees for their hospitality. We also thank Cedric Bailly, Jocelyn  
279 Barbarand, Thomas Blaise, Benjamin Brigaud, Yves Missenard, and Bertrand Saint-Bezar,  
280 members of the Relief, Bassins et Ressources (RBR) group at GEOPS, Université Paris-Saclay, for  
281 their insightful discussions on this topic. Additionally, we acknowledge Giovanni Camanni for  
282 reviewing an earlier version of this manuscript and Philippe Boulvais for providing insights into



283 fluid-rock interactions. We thank one anonymous reviewer and Stefano Tavani for their useful  
284 comments and Alexandra Tamas for editorial handling.

285

## 286 **Open Research - Availability Statement**

287 A textured 3D virtual outcrop model (VOM) of the studied outcrop is available for exploration  
288 and download on the Sketchfab repository at: <https://skfb.ly/pqSwC>.

289

## 290 **References**

- 291 Agosta, F., Alessandroni, M., Antonellini, M., Tondi, E. and Giorgioni, M., 2010. From fractures  
292 to flow: A field-based quantitative analysis of an outcropping carbonate reservoir.  
293 *Tectonophysics*, 490(3-4), pp.197-213.
- 294 Balsamo, F., Bezerra, F.H.R., Vieira, M.M. and Storti, F., 2013. Structural control on the  
295 formation of iron-oxide concretions and Liesegang bands in faulted, poorly lithified Cenozoic  
296 sandstones of the Paraíba Basin, Brazil. *Bulletin*, 125(5-6), pp.913-931.
- 297 Bear, J., Tsang, C.F. and De Marsily, G., 2012. *Flow and contaminant transport in fractured rock*.  
298 Academic Press.
- 299 Bergerat, F., Elion, P., De Lamotte, D.F., Proudhon, B., Combes, P., André, G., Willeveau, Y.,  
300 Laurent-Charvet, S., Kourdian, R., Lerouge, G. and d'Estevou, P.O., 2007. 3D multiscale  
301 structural analysis of the eastern Paris basin: the Andra contribution. *Mém. Soc. Géol. France*,  
302 178, pp.15-35.
- 303 Böcker, J., Littke, R. and Forster, A., 2017. An overview on source rocks and the petroleum  
304 system of the central Upper Rhine Graben. *International Journal of Earth Sciences*, 106, pp.707-  
305 742.
- 306 Bourbiaux, B., 2010. Fractured reservoir simulation: a challenging and rewarding issue. *Oil &*  
307 *Gas Science and Technology—Revue de l'Institut Français du Pétrole*, 65(2), pp.227-238.
- 308 Brigaud, B., Durllet, C., Deconinck, J. F., Vincent, B., Pucéat, E., Thierry, J., & Trouiller, A. (2009).  
309 Facies and climate/environmental changes recorded on a carbonate ramp: a sedimentological

310 and geochemical approach on Middle Jurassic carbonates (Paris Basin, France). *Sedimentary*  
311 *Geology*, 222(3-4), 181-206.

312 Bril, H., Velde, B., Meunier, A. and Iqdari, A., 1994. Effects of the “pays de bray” fault on fluid  
313 paleocirculations in the Paris basin dogger reservoir, France. *Geothermics*, 23(3), pp.305-315.

314 Cooke, M.L., Simo, J.A., Underwood, C.A. and Rijken, P., 2006. Mechanical stratigraphic controls  
315 on fracture patterns within carbonates and implications for groundwater flow. *Sedimentary*  
316 *Geology*, 184(3-4), pp.225-239.

317 De Dreuzy, J.R., Méheust, Y. and Pichot, G., 2012. Influence of fracture scale heterogeneity on  
318 the flow properties of three-dimensional discrete fracture networks (DFN). *Journal of*  
319 *Geophysical Research: Solid Earth*, 117(B11).

320 Delogkos, E., Roche, V. and Walsh, J.J., 2022. Bed-parallel slip associated with normal fault  
321 systems. *Earth-Science Reviews*, 230, p.104044.

322 Dershowitz, W.S. and Herda, H.H., 1992, June. Interpretation of fracture spacing and intensity.  
323 In *ARMA US rock mechanics/geomechanics symposium* (pp. ARMA-92). ARMA.

324 Filipponi, M., Jeannin, P.Y. and Tacher, L., 2010. Understanding cave genesis along favourable  
325 bedding planes. The role of the primary rock permeability. *Zeitschrift für Geomorphologie.*  
326 *Supplementband*, 54(2), p.91.

327 Frumkin, A., Langford, B., Lisker, S. and Amrani, A., 2017. Hypogenic karst at the Arabian  
328 platform margins: Implications for far-field groundwater systems. *Bulletin*, 129(11-12), pp.1636-  
329 1659.

330 Golab, J.A., Smith, J.J., Clark, A.K. and Morris, R.R., 2017. Bioturbation-influenced fluid pathways  
331 within a carbonate platform system: the Lower Cretaceous (Aptian–Albian) Glen Rose  
332 Limestone. *Palaeogeography, Palaeoclimatology, Palaeoecology*, 465, pp.138-155.

333 Grare, A., Lacombe, O., Mercadier, J., Benedicto, A., Guilcher, M., Trave, A., Ledru, P. and  
334 Robbins, J., 2018. Fault zone evolution and development of a structural and hydrological  
335 barrier: the quartz breccia in the Kiggavik Area (Nunavut, Canada) and its control on uranium  
336 mineralization. *Minerals*, 8(8), p.319.

- 337 Healy, D., Rizzo, R.E., Cornwell, D.G., Farrell, N.J., Watkins, H., Timms, N.E., Gomez-Rivas, E. and  
338 Smith, M., 2017. FracPaQ: A MATLAB™ toolbox for the quantification of fracture patterns.  
339 *Journal of Structural Geology*, 95, pp.1-16.
- 340 Lei, Q., Latham, J.P. and Tsang, C.F., 2017. The use of discrete fracture networks for modelling  
341 coupled geomechanical and hydrological behaviour of fractured rocks. *Computers and*  
342 *Geotechnics*, 85, pp.151-176.
- 343 Lopez, S., Hamm, V., Le Brun, M., Schaper, L., Boissier, F., Cotiche, C. and Giuglaris, E., 2010. 40  
344 years of Dogger aquifer management in Ile-de-France, Paris Basin, France. *Geothermics*, 39(4),  
345 pp.339-356.
- 346 Manzocchi, T., 2002. The connectivity of two-dimensional networks of spatially correlated  
347 fractures. *Water Resources Research*, 38(9), pp.1-1.
- 348 Mauldon, M., Dunne, W.M. and Rohrbaugh Jr, M.B., 2001. Circular scanlines and circular  
349 windows: new tools for characterizing the geometry of fracture traces. *Journal of structural*  
350 *geology*, 23(2-3), pp.247-258.
- 351 McGinnis, R.N., Ferrill, D.A., Morris, A.P., Smart, K.J. and Lehrmann, D., 2017. Mechanical  
352 stratigraphic controls on natural fracture spacing and penetration. *Journal of Structural*  
353 *Geology*, 95, pp.160-170.
- 354 Mégrien, C., 1980. Synthèse géologique du Bassin de Paris, I, Stratigraphie et paléogéographie.  
355 In: *Mémoires du Bureau de Recherches Géologiques et Minières*, vol. 101, 466 pp.
- 356 Moore, J.P. and Walsh, J.J., 2021. Quantitative analysis of Cenozoic faults and fractures and  
357 their impact on groundwater flow in the bedrock aquifers of Ireland. *Hydrogeology Journal*,  
358 29(8), pp.2613-2632.
- 359 Nelson, R.A., 1985. *Geologic analysis of naturally fractured reservoirs (Vol. 1)*. Gulf Professional  
360 Publishing.
- 361 Noufal, A. and Obaid, K., 2017, November. Bedding Corridors as Migration Pathways in Abu  
362 Dhabi Fields. In *Abu Dhabi International Petroleum Exhibition and Conference (p.*  
363 *D011S003R003)*. SPE.
- 364 Odling, N.E., Gillespie, P., Bourguine, B., Castaing, C., Chiles, J.P., Christensen, N.P., Fillion, E.,  
365 Genter, A., Olsen, C., Thrane, L. and Trice, R., 1999. Variations in fracture system geometry and

366 their implications for fluid flow in fractures hydrocarbon reservoirs. *Petroleum Geoscience*,  
367 5(4), pp.373-384.

368 Pomerol, C., 1978. Paleogeographic and structural evolution of the Paris Basin, from the  
369 Precambrian to the present day, in relation to neighboring regions. *Geologie En Mijnbouw*  
370 *Journal of Geosciences*, 57, pp.533-543.

371 Renshaw, C.E. and Pollard, D.D., 1995, April. An experimentally verified criterion for  
372 propagation across unbounded frictional interfaces in brittle, linear elastic materials. In  
373 *International journal of rock mechanics and mining sciences & geomechanics abstracts* (Vol. 32,  
374 No. 3, pp. 237-249). Pergamon.

375 Roded, R., Langford, B., Aharonov, E., Szymczak, P., Ullman, M., Yaaran, S., Lazar, B., Frumkin,  
376 A., 2024. Hypogene speleogenesis in carbonates by cooling, confined hydrothermal flow: The  
377 case of Mt. Berenike caves, Israel. *International Journal of Speleology*, 53(2), 191-209.

378 Sanderson, D.J., 1982. Models of strain variation in nappes and thrust sheets: a review.  
379 *Tectonophysics*, 88(3-4), pp.201-233.

380 Sanderson, D.J. and Nixon, C.W., 2015. The use of topology in fracture network  
381 characterization. *Journal of Structural Geology*, 72, pp.55-66.

382 Sauro, F., Zampieri, D. and Filipponi, M., 2013. Development of a deep karst system within a  
383 transpressional structure of the Dolomites in north-east Italy. *Geomorphology*, 184, pp.51-63.

384 Skurtveit, E., Torabi, A., Sundal, A. and Braathen, A., 2021. The role of mechanical stratigraphy  
385 on CO<sub>2</sub> migration along faults—examples from Entrada Sandstone, Humbug Flats, Utah, USA.  
386 *International Journal of Greenhouse Gas Control*, 109, p.103376.

387 Tanner, P.G., 1989. The flexural-slip mechanism. *Journal of Structural Geology*, 11(6), pp.635-  
388 655.

389 Thomas, H., Brigaud, B., Blaise, T., Saint-Bezar, B., Zordan, E., Zeyen, H., Andrieu, S., Wennberg,  
390 O.P., Casini, G., Jonoud, S. and Peacock, D.C., 2016. The characteristics of open fractures in  
391 carbonate reservoirs and their impact on fluid flow: a discussion. *Petroleum Geoscience*, 22(1),  
392 pp.91-104.

393 Vincent, B., Chirol, H., Portier, E. and Mouche, E., 2021. Contribution of drone photogrammetry  
394 to 3D outcrop modeling of facies, porosity, and permeability heterogeneities in carbonate  
395 reservoirs (Paris Basin, Middle Jurassic). *Marine and Petroleum Geology*, 123, p.104772  
396 Wilson, C.E., Aydin, A., Karimi-Fard, M., Durlofsky, L.J., Amir, S., Brodsky, E.E., Kreylos, O. and  
397 Kellogg, L.H., 2011. From outcrop to flow simulation: Constructing discrete fracture models  
398 from a LIDAR survey. *AAPG bulletin*, 95(11), pp.1883-1905.  
399 Zhu, W., Khirevich, S. and Patzek, T.W., 2021. Impact of fracture geometry and topology on the  
400 connectivity and flow properties of stochastic fracture networks. *Water Resources Research*,  
401 57(7), p.e2020WR028652.